

Richard F. Spaide

The main structural element of the eye is the sclera, a tough, translucent fibrous coat that provides a set shape and volume of the eye and functions as a protective casing for its fragile internal contents. The sclera is a composite of an interwoven network of collagen fibers (mostly type I) embedded in a hypocellular ground substance matrix. The sclera has some similarities to a pneumatic tire. The collagen fibers are analogous to the plies in a tire; they are relatively less distensible fibers embedded in a matrix that is more distensible. A pneumatic tire is inflated by air, while the sclera is inflated by the intraocular pressure. The mechanical engineering advantages of this arrangement include strength, sufficient rigidity without brittleness, and little need for intrinsic blood supply or cellular turnover. Because the eye has structural rigidity, its length and shape are not altered with eye movement. On the other hand the eye is easily deformable without suffering internal or external damage during ordinary use in life. Blood vessels and nerves of various sizes penetrate the sclera, and design features of the scleral openings help mitigate against loss of the intraocular contents. The muscles of the iris and ciliary body attach to the sclera as do the extraocular muscles used for movement of the globe. The sclera, which accounts for more than 90 % of the surface area of the eye [1], merges anteriorly with the optically clear specialization, the cornea.

Many changes occur in the sclera of high myopes, and these changes and the abnormalities they may induce are the focus of this chapter. In most high myopes the eye undergoes normal development in utero and early childhood to be followed later by progressive scleral thinning and ocular expansion. With knowledge of the base anatomy and the induced alterations caused by the expansion, the subsequent

abnormalities associated with myopia are easier to understand. As such this chapter starts with a review of the embryology and development of the sclera, its anatomy, and mechanical properties. Features of what happens in myopization will then be presented, followed by how these forces cause specific clinically recognizable alterations in the sclera and associated structures. One specific and important induced alteration, the staphyloma, is sufficiently complex as to require treatment in its own accompanying chapter entitled, creatively enough, “Staphyloma.”

8.1 Embryology and Development of the Sclera

The evagination of the optic vesicle starts in the fourth week and invaginates to form the optic cup in the fifth week. A thickening of the overlying ectoderm called the lens placode develops around this time and will eventually invaginate to form the primordial lens. The sclera is derived from the neural crest and, to a much lesser extent, the mesoderm, starting in the sixth week as waves of invading cells form a condensation on the optic cup (Fig. 8.1). It appears that the pigment epithelium and the uvea are required to induce formation of the posterior sclera. Incomplete closure of the fetal fissure causes colobomas to occur, and these colobomas influence development of the nascent sclera. The sclera develops anterior to posterior but also in an inner to outer scleral vector as well [2]. Over the next months the thickness of the collagen fibers increases so that by week 24 the fibers are three times thicker than they were at week 6.2. In a normal eye the anterior sclera reaches adult size by age 2, while the posterior sclera does so by age 13. The axial length of a term infant is about 17 mm and is destined to reach 23 mm by age 13 years [3]. Considered as a simple sphere, the eye expands 2.5 times in volume over this time. The remarkable aspect of ocular growth is that the eye can remain emmetropic even though the individual components of the eye are growing at their own individual rate.

R.F. Spaide, MD
Vitreous, Retina, Macula Consultants of New York,
460 Park Ave, 5th Floor, New York,
NY 10021, USA
e-mail: rickspaide@gmail.com

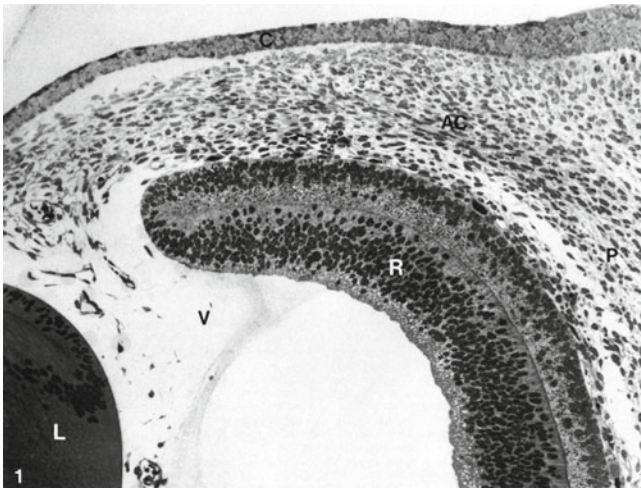


Fig. 8.1 At week 6.4 there is a condensation of mesenchyme (AC) around the optic cup. The cell density in the mesenchyme is somewhat lower posteriorly (P) in this section. The retina (R) is undergoing differentiation and is in contact with the vitreous (V). The lens (L) is visible at the bottom left (Derived from Sellheyer and Spitznas [2])

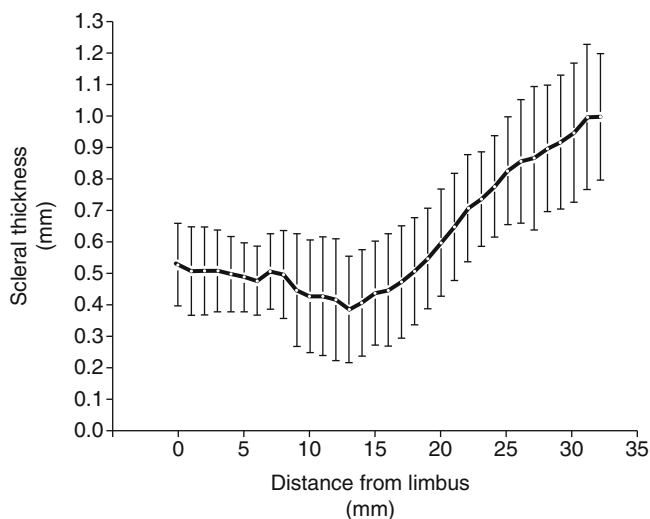


Fig. 8.2 Graphical representation of the scleral thickness in normal eyes extending from the surgical limbus (*left*) toward the optic nerve (*right*) (Derived from Olsen et al. [1])

8.2 Gross Scleral Anatomy of an Emmetropic Eye

In an emmetropic eye the sclera shell has a diameter of approximately 24 mm and a surface area of approximately 17 cm² [1]. The sclera has no lymphatics or cellular boundary. The thickness of the sclera in a non-myopic eye varies considerably with location; the thickest is around the optic nerve where it can be slightly more than 1 mm, while immediately under the rectus muscle, insertions it can be as little as 0.3 mm thick. In the submacular region the sclera has a thickness of about 0.9 mm in normal eyes (Fig. 8.2). On the

outer surface of the scleral stroma is the episclera, a loose connective tissue. Anteriorly the episclera contains a plexus of capillaries, but no lymphatics. The sclera is enveloped by Tenon's capsule, a double layer of fibrous tissue with a smooth inner border separated from the eye by a potential space occasionally traversed by diaphanous strands of the episclera [4]. Tenon's capsule merges with the dura mater of the optic nerve posteriorly and the muscle capsules. The inner surface of the sclera is composed of a thin layer containing melanocytes giving it a brown color and its name, lamina fusca.

The anterior portion of the sclera terminates at the posterior boundary of the cornea at what is called the anterior scleral foramen. The limbus forms the transitional zone between the sclera and the cornea. The largest opening in the sclera posteriorly is the scleral canal, which exists to allow exit of the optic nerve. The retinal nerve fiber layer changes direction by bending around the inner opening of the optic canal, formed by Bruch's membrane and the scleral ring to head posteriorly out of the eye. The inner opening of the optic canal is approximately 1.8 mm in diameter. Somewhat anterior to the midpoint of the optic canal, there is a sievelike network of fibers, called the lamina cribrosa, which criss-cross the breadth of the canal. The openings, or pores, are bordered by these fibers within each plate of the lamina. The pores in an emmetropic nonglaucomatous eye are round or oval, and the pores are nearly aligned in a vertical sense from one plate to another, except toward the periphery of the lamina cribrosa. The resultant openings allow the nerve fibers to exit the eye. A central opening in the lamina is larger than the surrounding to allow passage of the central retinal artery and vein. The pores in the lamina are largest superiorly and inferiorly, where the predominate number of nerve fibers are seen to enter the optic canal [5]. Providing additional structural and metabolic support in this region are the closely associated glial cells [6, 7]. Surrounding the optic nerve as it transits the lamina is the border tissue of Elschnig. The diameter of the canal increases posteriorly to accommodate the larger diameter of the retrolaminar optic nerve, which contrary to the prelaminar portion of the optic nerve is myelinated. The posterior optic nerve canal is approximately 3.5 mm wide. The optic nerve has a dura mater covering. The outer two-thirds of the scleral collagen merge with the fibers of the dura mater.

Arteries, vein, and nerves course through smaller openings in the sclera. These openings, or emissaries, are often placed at an angle to the thickness of the sclera, apparently to reduce the likelihood of loss of intraocular contents with increased pressure in the eye. The 15–20 short posterior artery emissaries aggregate around the optic nerve and macular regions. Using optical coherence tomography (OCT) with deeper imaging capabilities, it is common to see branching of some of the posterior vessels in the sclera. Therefore there are at least as many internal openings of the emissaria as

there are external openings in the sclera. Most of the emissaries in the posterior pole are for the short posterior ciliary arteries to bring blood flow into the choroid. Branches from short posterior ciliary arteries, with possible contributions from the choroidal circulation, form a ring, often incomplete, around the prelaminar portion of the optic nerve known as the circle of Zinn-Haller. This circle is located a mean of 403 μm from the outer portion of the optic nerve in normal eyes. The mean vascular diameter was 123 μm but ranged from 20 to 230 μm in diameter [7]. There is variation to the depth that the circle of Zinn-Haller is located but may be as much as 345 μm below the inner scleral surface [8]. This structure reportedly is visible with angiography [9, 10]. The long posterior ciliary arteries enter the sclera nasal and temporal to the optic nerve and do not fully penetrate the inner portion of the sclera until the equator. The main venous drainage of the choroid occurs through the vortex veins, the ampullae of which are found at the equator of the eye. The vortex veins travel obliquely through the sclera to exit the eye posterior to the equator. Associated with the insertions of the rectus muscles are the anterior ciliary arteries, which bring blood flow to the ciliary body. Superficial branches of these arteries contribute to the episcleral circulation. There is also a copious supply of nerves as evidenced by the pain associated with trauma or inflammation of the sclera.

8.3 Fine Anatomy of the Sclera

The sclera is composed of collagen fibers of varying sizes, but the inner fibers are smaller, about 62 nm, than the outer fibers, which are about 125 nm [11] (Fig. 8.3). The fibrils are composed of type I collagen and consequently have high proportions of proline, hydroxyproline, and hydroxylysine. The presence of hydroxylysine provides for the possibility of molecular cross-linking, which increases the tensile strength and mechanical stability of the sclera. These structural modifications can come at the expense of increased rigidity. The collagen fibers are embedded in interfibrillary matrix composed of proteoglycans. Proteoglycans have a protein core that is attached to varying numbers of glycosaminoglycans, which are long molecules composed of sugar subunits. Proteoglycans are classified by the nature of the core protein and by the number and types of attached glycosaminoglycans. The two main glycosaminoglycans in the sclera are chondroitin sulfate and dermatan sulfate, which alone or in combination contributes to the formation of the major proteoglycans, biglycan, aggrecan, and decorin [13]. The remarkable attribute of proteoglycans, conferred by their glycosaminoglycan constituents, is the ability to bind to large amounts of water. This allows proteoglycan fraction to occupy large volumes with little dry weight. The predominant glycosaminoglycan appears to vary somewhat with topographical location in the sclera [14]. Estimates of the

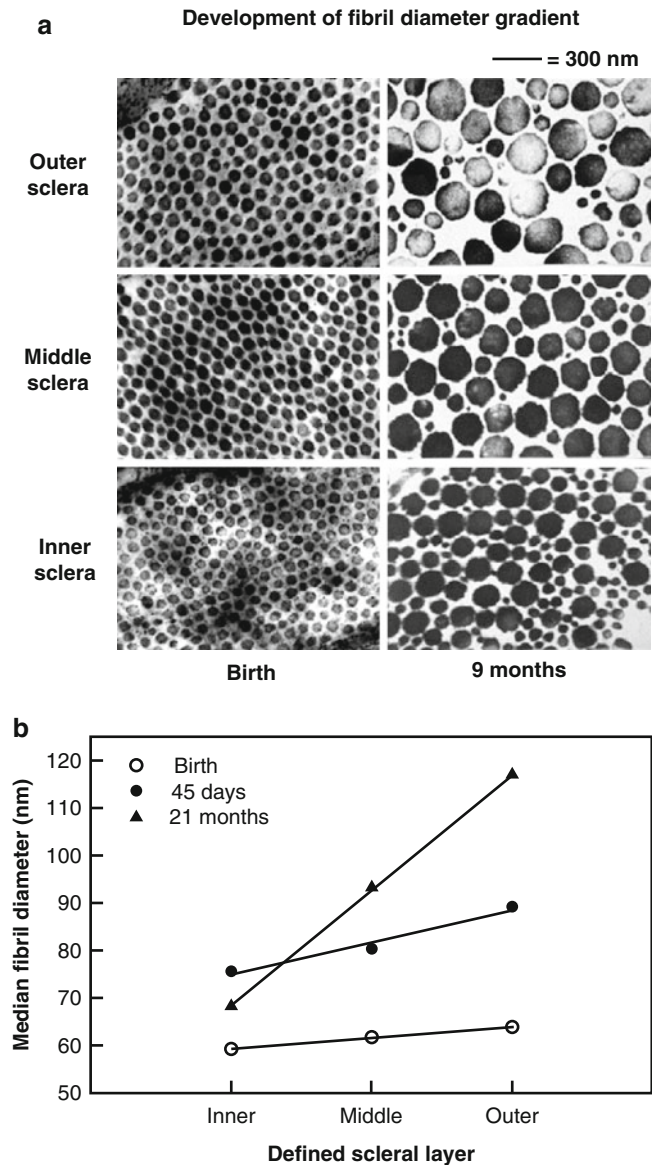


Fig. 8.3 (a) The cross-sectional thickness of collagen fibers in the outer, middle, and inner sclera at birth and at 9 months. (b) The median cross-sectional diameter is shown graphically at birth, 45 days, and 21 months for the tree shrew (Derived from McBrien et al. [12])

proportions of the constituent parts of the sclera vary, but as a rough guide the sclera is composed of roughly 68 % water, 24 % collagen, 1.5 % elastin, 1.5 % proteoglycans, and the remainder fibroblasts, nerve tissue, blood vessels, and salts. The inner surface of the sclera, the lamina fusca, has a large number of elastin fibers [15]. Elastin has a high proportion of hydrophobic amino acids and contains a low proportion of hydroxyproline and hydroxylysine. It does have desmosine, which is a derivative of lysine and is used to make cross-links between elastin fibers. Also contained within the sclera are matrix metalloproteinases, which are enzymes that are capable of degrading proteoglycans and collagen. These enzymes are stored in an inactive form and can be activated during inflammation and growth.

The cores of the lamina cribrosa fibers are composed of elastin surrounded by collagen fibers. Encircling the optic nerve in the region of the lamina are layers of concentrically arranged elastin fibers [16]. At the outer surface of the elastin fibers, ring merges into the sclera. Elastin fibers of the lamina merge into the inner portion of the surrounding elastin fibers. Glial cell processes extend from the lamina cribrosa into the concentric elastin fibers and also appear to help anchor the lamina. The arrangement of elastic fibers would seem to serve as a buffer against trauma from rapid changes in intraocular pressure. On the other hand the layered arrangement could lead to the possibility that a dehiscence or separation of the layers could occur.

A number of molecular changes happen in the sclera with age. The cross-linking between adjacent collagen fibers increases, and so does glycosylation and accumulation of advanced glycation end products [17]. There is a decrease in the amount of type I collagen present, the diameters of the collagen fibers increase, and there is a greater variability in the sizes of the fibers with age [18] (Fig. 8.3). The amount of decorin and biglycan decreases with age, as does sclera hydration [19, 20]. There is a decrease in the amount of elastin with age. These contribute to the altered biomechanical characteristics of the sclera with age, particularly an increase in stiffness [20–23]. The amount of collagen in the lamina cribrosa increases, as does the cross-linked proportion [24].

As compared with the transparent cornea, the white relatively opaque nature of the sclera is related to the more randomly oriented and larger diameter collagen fibers and the greater amount of water bound. A common occurrence in retinal detachment surgery is a localized drying of the sclera allowing some visualization of the underlying choroid. With rehydration the sclera becomes whiter and less translucent.

8.4 Mechanical Properties of the Sclera

The sclera is a viscoelastic substance. Over smaller ranges of tensile pulling, or stress, a sample of sclera will lengthen or show strain [25] (Fig. 8.4). Release of the stress after a short period of time leads to a recoil in the length of the sample. The same load applied over a longer period of time will result in more tissue extension than just the elastic stretching. The difference over time is called creep rate of a viscoelastic tissue (Fig. 8.5). A commonly seen practical example of the viscoelastic properties of sclera is shown by how the height of a scleral buckle will seem to increase over days following surgery. The initial buckling effect is from the elastic strain, while the increase in size of the buckling effect in the subsequent days is due to a slower creep of the viscoelastic sclera.

The relationship between stress and strain provides a measure of the stiffness of a material. The sclera shows

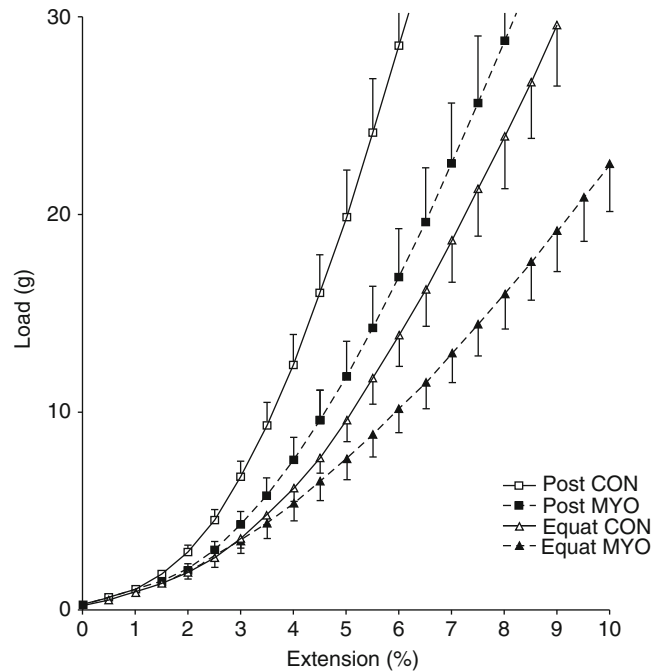


Fig. 8.4 The elastic properties of the sclera. The amount of expansion (strain) for increasing amounts of load (stress) is shown graphically for the control normal strips (*CON*) and the myopic eyes (*MYO*) for both the posterior pole (*Post*) and the equatorial region (*Equat*) (Derived from McBrien et al. [12])

increasing stiffness with age. In babies the sclera is highly distensible. The newborn's eye can expand and adopt a bovine appearance from congenital glaucoma (buphthalmos – which means “ox eye”). Over life the sclera loses some of its dispensability, and interestingly the change in stiffness is highly dependent on location in the eye. In a study by Geraghty et al., the change in stiffness with age of the anterior sclera was much more pronounced than the posterior sclera, and the change was statistically significant only for the anterior sclera [21]. Pressure loading of the eye appears to cause a variable amount of stiffness increase in eyes.

The biomechanical behavior of the posterior sclera to increased pressure shows variation from one person to the next but is nonlinear and anisotropic [26]. Experiments on isolated eyeballs may overstate some induced biomechanical properties of the eye because under ordinary circumstances the eye is suspended in extraocular tissue, which has a pressure of its own. The extraorbital pressure is estimated as being about 20 % of the intraocular pressure. That means the pressure gradient across the sclera is lower than the intraocular pressure posteriorly within the orbit, but not anteriorly along the external surface of the eye.

The main source of resistance of passage of both water and larger molecules through the cornea is the corneal epithelium [27]. The corneal endothelium is also a source of

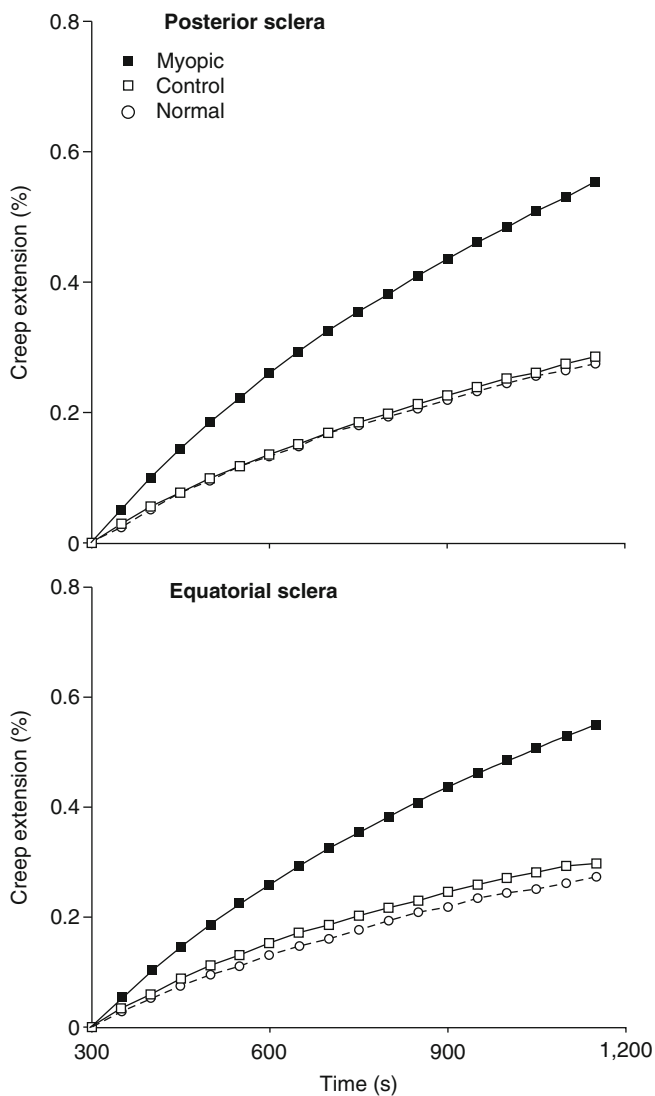


Fig. 8.5 The viscoelastic properties of sclera. With a constant applied load, the sclera will show increasing amounts of strain over time. This slow extension is called creep. Note the increased amount of creep for myopic samples as compared with normal or contralateral control eyes. The *top graph* is the posterior pole and the *bottom* for sclera strips obtained from the equator (Derived from McBrien et al. [12])

resistance albeit quite a bit lower than the corneal epithelium. The sclera has neither an epithelium nor endothelium and consequently is quite permeable to the flow of water and larger molecules through its substance [28, 29]. Contained within the eye is the choroid, which is a densely packed permeable layer of blood vessels without a lymphatic system. Consequently protein, fluid, and other intravascular elements that have leaked into the extravascular space in the choroid not removed by reabsorption by the choroidal vessels are removed by diffusion posteriorly through the sclera into Tenon's space.

The scleral stroma receives oxygen and nutrition externally from the episclera and Tenon's capsule externally. An

interesting possibility is the stroma receives oxygen from the choroid internally. The passive diffusion of proteins and the like from the choroidal circulation may serve as a source of metabolic building blocks for the few stromal fibroblasts present. The amount of fluid requiring drainage is probably related to the thickness of the choroid and the permeability of the vessels in the choroid. The resistivity to flow out through the sclera is likely to depend on thickness and exact composition of the sclera itself. In eyes with uveal effusion syndrome, the choroid is thick, as is the sclera [30]. The collagen fibril diameters are larger and more variable [31], and there appears to be decreased diffusion of larger molecular weight substances such as albumin through the sclera in eyes with uveal effusion [32]. When areas of sclera are excised from the sclera such that the remaining thickness is a fraction of the original thickness, fluid can be seen to seep through the window created.

8.5 Emmetropization and Myopization

The axial length of the eye increases by about 35 % from infancy to adulthood [3, 33], and the individual components of the eye that have an effect on refractive error change at slightly different rates [34–37]. Each of these components eventually adopts a Gaussian distribution. Even though the pooled variance is expected to be a Gaussian distribution as a function of all of the individual variances, the measured refractive errors actually show a peaked, or leptokurtic, distribution with far too many eyes having emmetropia or slight hyperopia. Although the individual components vary, they all work together in concert to achieve an eye that has little refractive error in most cases. The obvious exception is that the curve shows a skew toward myopic refractive errors. Although emmetropization is amazing, it is a logical consequence of evolutionary pressures: if vision is an advantageous thing, then good vision is even more so.

The process of emmetropization appears to be an active process that is largely mediated by changes in the choroid and sclera [38] (Fig. 8.6). Occlusion, form deprivation, and imposition of refractive lenses all cause alterations in the refractive capabilities of animal eyes after birth. Form-deprivation and lens-induced refractive change has been demonstrated in animals ranging from fish, chick, kestrel, squirrel, mouse, guinea pig, cat, and tree shrew to monkey and appears to be true in humans as well [39–56]. The first changes include alterations in the thickness of the choroid [54, 57–59]. In eyes becoming more myopic, the choroid becomes thinner as compared to those eyes becoming hyperopic. Removal of the stimulus stops the induced alteration in refractive error. The choroid thickness change normalizes, and the direction of the choroidal thickness change is always in the correct direction [57–60].

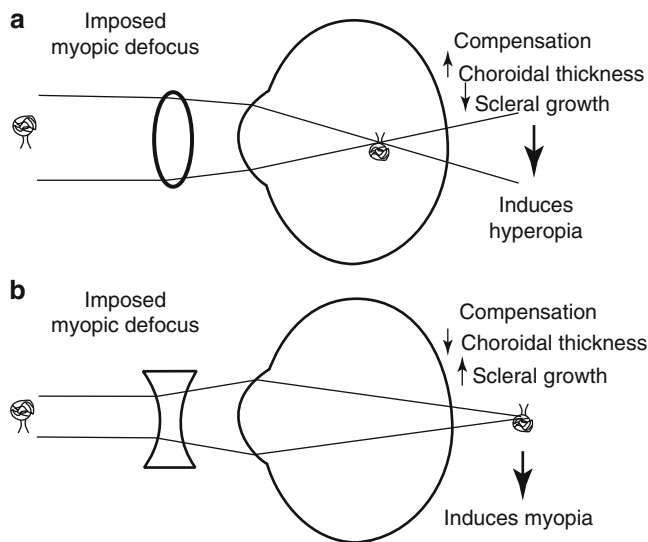


Fig. 8.6 The compensatory changes induced by forced wearing of spectacle refraction as evidence of active emmetropization. **(a)** Forced wearing of a plus lens brings the image plane in front of the retina. In compensation the eye shows increased choroidal thickness. In birds this can be dramatic and can account for one-half of the early compensatory response. Eventually there is a decrease in scleral growth rate. **(b)** A negative lens shifts the focal plane behind the retina and the eye shows decreased choroidal thickness and scleral remodeling to include increased growth of the posterior sclera. In each case the eye changes in character to move the level of the retina toward the focal plane of the combined lens and dioptric mechanism of the eye. In addition, removal of the spectacle lens leads to the exact opposite of the induced effects to occur. For example, removing the plus lens will cause the choroid to become thinner and the eye to expand toward its normal size [38]

Longer-term application of either form-deprivation or lens-induced errors is followed by axial length changes of the eye, shortening in the case of hyperopia and lengthening in the case of myopia (Fig. 8.7). These changes are also reversible in that removal of the stimulus causes an acceleration or retardation in the growth of the eye to the extent it approaches emmetropia over time. Optic nerve sectioning or destruction of the ciliary nerve does not prevent the development of experimental myopia [40, 42, 61]. Form deprivation of a hemifield produces expansion of the eye conjugate with that hemifield [55, 62, 63]. These findings all support a hypothesis that remodeling of the eye occurs due to local effects within the eye starting with signaling that originates in the retina and choroid that eventually affects the sclera.

Experimental myopia induces several changes in the composition of the sclera. There is a general loss of collagen and proteoglycans. With the start of experimental myopia, there is a reduction in ongoing type I collagen synthesis, and existing collagen and proteoglycans are degraded by matrix metalloproteinases [64–66]. After a significant amount of myopia has developed, the collagen fibril diameter decreases, particularly in the outer portions of the sclera [64]. The decreased and altered collagen appears to be responsible for

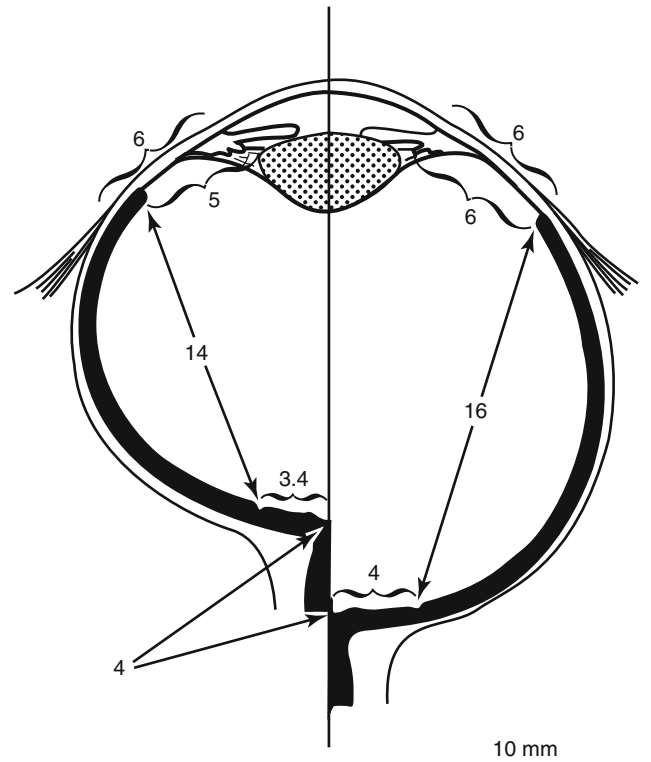


Fig. 8.7 Eye lid fusion in monkeys causes an expansion of the posterior sclera (*right side* as compared with the normal *left*), but virtually no change in the anterior segment (From Wiesel and Raviola [52])

changes in the biomechanical characteristics of the sclera [12, 67]. Myopic sclera shows more elasticity and greater viscoelastic creep over time (Figs. 8.3 and 8.4). This could suggest passive expansion of the eye occurs as the result of intraocular pressure. However administration of timolol decreased intraocular pressure but did not affect the development of myopia in a chick model [68]. This implies there may be a control mechanism that drives the amount of axial lengthening and thereby the amount of myopia.

8.6 Human Myopia

Myopia seen from an epidemiological standpoint is an increasing problem related to modern society. Sweeping changes in the pattern of refractive error have been seen in populations changing from agrarian to urban-based living [69–73]. Urban children spend more time indoors occupied with near activities and less time outdoors [74–77]. Eskimo populations showed shift of refractive error from hyperopic to myopic in the early and mid-twentieth century coincident with the introduction of schooling [78, 79]. Although there is a modest inheritable effect for myopia [80], the strongest predictors of developing myopia appear to be near work and decreased time spent outdoors when young [75, 77].

The time outdoors exposes the eye to a reduced dioptric range and also to increased amounts of shorter wavelength light as compared with indoor lighting.

The development of high myopia seems to be driven by processes related to emmetropization with the less desirable effect of producing a radically incorrect refractive error – for distance acuity that is. On the other hand close work as a risk factor would seem to be an adaptive mechanism. The receptive part of the eye is being shifted to the most common focal plane of the eye. Because close work has been associated with accommodation, the idea of preventing accommodation as a way of decreasing the progression of myopia has been considered for more than a century. In 1876 Loring discussed possible mechanisms by which myopia could develop and the potential pharmacotherapeutic effects of atropine in a very interesting review [81]. In 1891 Taylor recommended atropine, blue glasses, and leaches as a treatment of progressive myopia [82]. In 1979 Bedrossian reported eyes treated with atropine were less likely to show progression of myopia as compared with untreated eyes [83]. McBrien and coworkers more recently demonstrated atropine could blunt the development of form-deprivation myopia in a mechanism that was independent of accommodation [84].

In the process of myopization in humans, there is expansion of the posterior sclera and expansion of the vitreous cavity. Associated with the increasing myopia is thinning of the choroid [85–87], but as was seen in animal models, thinning of the choroid precedes scleral enlargement. There does seem to be control mechanisms involving the sclera that are mediated by or at least are influenced by the choroid. This raises the question: do abnormalities of the choroid contribute to the progression of myopia? This is an important question given the potential for undesirable feedback loops to occur in progressive myopia. Indeed, myopia is a common association with many diseases that affect the choroid or retina and then secondarily the choroid such as choroideremia, gyrate atrophy, retinitis pigmentosa, congenital stationary night blindness, Kearns-Sayre syndrome, progressive bifocal chorioretinal atrophy, achromatopsia, and fundus flavimaculatus [88–95]. With increasing myopia the choroid ordinarily becomes quite thin and can disappear in patches altogether. Eventually the patches become larger and confluent resulting in broad white areas of absent choroid, with a loss of the overlying retinal pigment epithelium and outer retina as well. These same eyes are often the ones with the most exaggerated findings in the sclera [96]. Whether or not relevant signaling originating from the choroid is correct when the choroid is in the last throes of existence is not known.

The expansion and stretching of the posterior pole induced in myopia affects every aspect of the sclera. The wall thickness decreases, the curvatures change, the emissary openings widen, and the scleral canal can enlarge, become tilted and

distorted. Local exacerbation of ocular expansion is manifested as regional outpouchings, staphylomas. In the following sections the clinical manifestations of these changes will be shown.

8.7 Ocular Shape

Along with location, rotation, and size, shape is one of the elemental features of an object. Shape can be difficult to describe, but the eye has a general ellipsoidal shape and therefore is potentially easier to model. The most exacting representation would be in the form of a mathematical statement, but mathematical equations are difficult to incorporate into everyday speech. Verbal simplifications of shape commonly have been substituted, sometimes to extent of ineffective oversimplification. In most publications the three-dimensional characteristics of the shape were reduced to cardinal planes for description and analysis. The analysis of these planes varied in sophistication from measuring linear distances and angles to fitting curves to the shapes. One common method of describing spheroids is to use the terms oblate and prolate. Oblate spheroids are obtained by rotating an ellipsoid along its minor axis. The resultant eye shape would be flatter in the posterior pole and would steepen toward the equator. The flatter side of an egg has an oblate shape. A prolate shape is obtained by rotating an ellipse along its major axis and thus is lengthened in the direction of its polar diameter. The pointy side of an egg has a prolate shape. There are two main approaches to estimate the shape of the eye. One method, which initially may seem to be the more precise and useful of the two, is to image the eye with a tomographic means such as with computed axial tomography or magnetic resonance imaging. The second way is to measure the refractive error and to make assumptions about the eye from these measurements. Widefield refractive error measurements may supply information that is more useful in regard to physiological processes that influence the development of myopia. The size estimates in these papers are of secondary importance since the refractive error across the expanse of the retina has been shown to have extremely important consequences as will be described below (Fig. 8.8).

Cheng and associates [97] obtained multislice magnetic resonance images and measured the diameters in the sagittal, coronal, and transverse planes. The eye shape for hyperopic and emmetropic eyes was similar, and both had a coronal diameter greater than the transverse or sagittal diameters. Myopes had the same basic eye shape but appeared to be larger in every radius. Atchison and coworkers [98] fitted symmetrical ellipsoids to the transverse and sagittal images of emmetropic and myopic eyes derived from magnetic resonance imaging. They found considerable variation in shape, but most emmetropes had an oblate shape, that is, one that

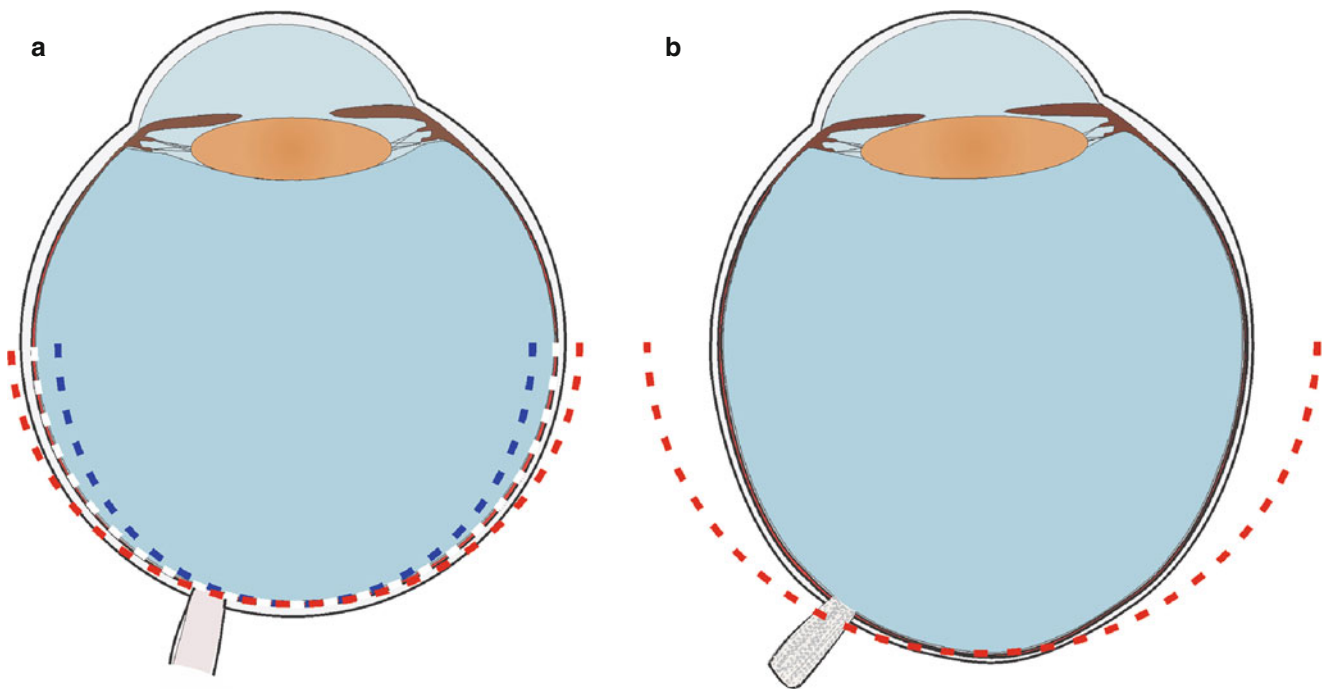


Fig. 8.8 (a) Shows the cross section of an emmetropic eye with its typical mild oblate shape. Three different image planes are shown by the dashed lines, all of which intersect the fovea posteriorly. The white dashed line falls on the peripheral retina as well. The blue dashed line demonstrates an image plane in which the periphery is relatively myopic as compared to the posterior pole. This is a common occurrence in emmetropes, particularly if there is accommodation. The red dashed line shows the image plane that falls behind the retinal surface in the

periphery. In this case the periphery is relatively hyperopic as compared with the posterior pole. (b) In highly myopic eyes the eye shape is more prolate. This causes an exaggerated amount of peripheral hyperopia, which is common in high myopes. The significance of this occurrence is in emmetropization, which seems to strike a balance minimizing the refractive error across the whole eye, even though we consider foveal vision to be the most important. The peripheral hyperopia may create a drive toward increasing myopization of the posterior pole

was flatter in the posterior pole. Myopes showed an increase in all dimensions with a loss of oblateness. Only a few of the myopic eyes demonstrated a frank prolate shape, however.

Lim and colleagues [99] looked at a subset of Singaporean Chinese boys enrolled in a population-based study in Singapore. Eye shape was assessed from 3-dimensional models, and the diameters along the cardinal axes were recorded. Myopic eyes were larger and had greater surface area, as would be expected. The eyes were larger along the longitudinal axial length and transverse diameter, but apparently not the vertical diameter in the coronal plane. The myopic eyes had a prolate profile in the axial plane. Thus even in younger individuals, the eyes appeared to have differing size and shape. Ohno-Matsui and associates [96] evaluated myopic eyes and divided the posterior curvature of the eye into four types. The first three types all appear to be variations on a prolate shape with the apex of the curve located at the optic nerve, the central macula, or just temporal to the center of the macula, but the presence or absence of staphylomas as an influencing characteristic was not stated. The fourth shape was termed irregular, because the curvature was not smooth. Eyes with irregular curvature were significantly older, had longer axial lengths, and were more likely to have myopic fundus lesions. It is not clear if the myopic fundus lesions

were primarily associated with the irregular shape or the increased axial length and age.

Tomographic means show the general shape of the eye, but to be able to determine regional refractive effects, the shape abnormalities could have would require knowledge of the corneal shape and the refractive powers of the crystalline lens in different meridians, which cannot be determined with sufficient accuracy from the tomographic images. Ordinary refractive evaluation and correction of the eye seeks to correct defocus and astigmatism of the image on the macula. That is, only the central acuity is optimized. An ideal lens in a camera system would form an image of a flat plane as a flat plane. With actual simple lenses the image formed is a curved image plane. The field curvature makes it difficult for a rigid flat sensor such as a digital sensor to produce a uniformly sharp image across this field. The eye has a curvature inherent in its anatomy so field curvature potentially is a desirable characteristic. The important consideration, of course, is if the field curvature of the dioptric mechanism of the eye matches the anatomic curvature of the eye (Fig. 8.8). In many emmetropic eyes the periphery is relatively myopic, and this relative myopia increases with accommodation [100]. In high myopia there is an axial lengthening of the eye so that there is an increasing difference between the distance

from the nodal point of the eye to the posterior pole as compared with the equatorial regions. This means the periphery is typically relatively hyperopic as compared with the posterior pole in high myopes, with the amount of relative hyperopia increasing with the increase in myopia because the eye does not expand symmetrically in axial myopia. As eyes become more prolate, the differences in refraction become more evident [101–106]. Relative hyperopia of the periphery has been documented in many large studies [101–109].

Animal models of myopia show that both defocus and form deprivation lead to myopia, even if the fovea is ablated [110–113]. After foveal ablation monkeys reared with occluders that caused form deprivation only in the periphery developed myopia to the same degree as animals not undergoing foveal ablation that still had peripheral occlusion [110]. Animals undergoing foveal ablation that were not hindered in emmetropization [111] and generalized form deprivation still caused myopia. The peripheral refractive errors were not different in eyes having foveal ablation as compared with those who did not [112]. Peripheral retinal defocus induced myopia even if there was foveal ablation [113]. These findings establish the importance of the periphery in the development of form-deprivation myopia. Chicks reared with concentric two zone lenses were evaluated for amount of emmetropization in the face of varying imposed refractions [114]. The posterior portion of the eye appeared to contribute to the overall refraction of the eye in proportion to its surface area. Summarizing this new information with what has already been presented in this chapter, the eye has local mechanisms that influence eye growth, but there appears to be some larger acting mechanisms that extend beyond these local regions to affect growth of the posterior portion of the eye. In terms of surface area, the periphery is the most important, but in everyday life refraction of the eye is optimized for the fovea. This same optical correction may then place the periphery at increased amount of hyperopic defocus. The drive toward emmetropization appears to involve the whole eye, weighing the periphery and posterior pole on a surface area basis. Therefore while the eye may be grossly large and the macula has a myopic refractive error, the periphery is still hyperopic because of the shape of the eye and field curvature (Fig. 8.8). This may compound the propensity to develop increasing amounts of myopia.

Because of the significance of the periphery in the development of axial myopia, some studies have tested the hypothesis that peripheral hyperopia may precede, or at least be predictive of, the development of axial myopia. The effect, if present, seems relatively small. Relative peripheral hyperopia was seen to precede the development of axial myopia in a prospective study over 8 years involving 605 children [104]. A study of 105 children over a period of 1.26 years did not find evidence of the same, although the

statistical power of this study was limited [115]. A larger study done by Mutti of 774 myopic children followed from Grades 1–8 found a modest predictive effect for myopia by peripheral hyperopia [109]. The risk appeared to vary by ethnic group. A limitation of this line of reasoning is the image quality in the periphery is a function of a number of features such as defocus, oblique astigmatism, spherical aberration, coma, and chromatic aberration [116–119]. It appears likely that peripheral image degradation contributes to the formation of myopia, but simple defocus is only one of many potential contributors to decreased image quality. Indeed the peripheral retina appears to weigh the amounts of image blur caused by radial versus tangential astigmatism as one means of providing a feedback signal [103, 120].

The shape of the eye, as manifested by scleral expansion, is at the heart of myopia. The experiments in animals are relatively recent in human scientific endeavors and are likely to hold the keys to unlocking many of the mysteries of myopia. Animal experiments may have limited utility as they apply to humans. If the fovea contributes to the signal modulating eye expansion in relation to its surface area, the periphery would be more important just because of area reasons alone. A second important point is humans, who depend extensively on fovea vision for reading and other close tasks, may differ from monkeys in the relative proportion that the periphery accounts for in the development of myopia. Of interest, though, is the list of chorioretinal conditions associated with myopia previously mentioned in this chapter was predominated by diseases that primarily affect the peripheral vision first. Thus evaluation of the peripheral visual function appears to be an important area for future myopia research.

8.8 Shape Alterations Across Smaller Units of Scale

After evaluating the general shape of the eye, the next lower unit of scale would be to evaluate regional variations. Large regional variations in eye shape usually are manifested as outpouchings of the eye. These outpouchings are known as staphylomas. The principle area affected by staphylomas is the same as that affected by general expansion of the eye, namely, the posterior portion of the eye. Ocular abnormalities associated with staphylomas include subretinal fluid [121, 122], choroidal neovascularization [123], polypoidal choroidal vasculopathy [124], retinal detachment [125], myopic macular schisis [126, 127], peripapillary intrachoroidal cavitation [128], macula intrachoroidal cavitation [129], pits [130], choroidal folds [131], and tilted optic nerve appearance. For the most part these topics are discussed in the chapter devoted to staphylomas. Tilting of the optic nerve will be covered in part here, but for the most part in the chapter “Optic Nerve.”

The nonuniform mechanical expansion of the eye shifts the plane of the optic nerve from pointing toward the geometric center of the vitreous cavity to point toward the nearest foci of the ellipse describing the shape of the posterior pole. Since the shape of the posterior portion of the eye in high myopia is prolate, the nerve shifts such that a normal to its surface points more posteriorly than what is seen in a myope. This causes the anterior edge to be forward of the posterior edge along a transverse plane than what would be seen in an emmetrope. This shifting of orientation is compounded by the frequent development of distension of the globe with coexistent atrophy of the choroid and retinal pigment epithelium by a roughly triangular-shaped area inferotemporal to the optic disc known as the conus.

The terminology used to describe tilted discs is suboptimal. There are three axes of rotation possible and in aviation each of the movements has a different name. As shown in Fig. 8.9, these are yaw, roll, and pitch. Translated to the eye tilting of the optic nerve usually corresponds to yaw. The long axis of the nerve may be rotated, usually with the top of the nerve being rotated temporally. This is often referred to as torsion of the nerve (corresponding to roll in an airplane), although often the term tilt is used to refer to both tilt and torsion. There is no commonly used term to signify the amount that the superior part of the nerve may be in front or behind the bottom portion, although the aviation term pitch seems perfectly usable.

The effects related to ocular expansion of the posterior segment may produce recognizable alterations on even smaller units of scale.

8.8.1 Ectasia of the Sclera and Intrasccleral Cavitations Related to Emissary Openings

With expansion of the eye, the sclera becomes thinner. Emissary vessels ordinarily penetrate the eye, often at oblique angles, and course through the sclera toward the choroid. With scleral thinning these passageways become much shorter. The internal openings of the emissary openings seem to become stretched and enlarged (Figs. 8.10, 8.11, and 8.12). Concurrently the structures supplied by arterioles, such as the choroid, thin and in some areas are obliterated. As a consequence the vessels that used to supply these structures also become attenuated. These emissary openings are evident as funnel-shaped depressions associated with threadlike vessels emanating from the deeper sclera. Because the course of the emissary passageway often is at a shallow angle to the sclera, the opening of the emissary itself can be tilted. These openings typically are noticed in the context of profound atrophy of the choroid, retinal pigment epithelium, and overlying retina. In some cases

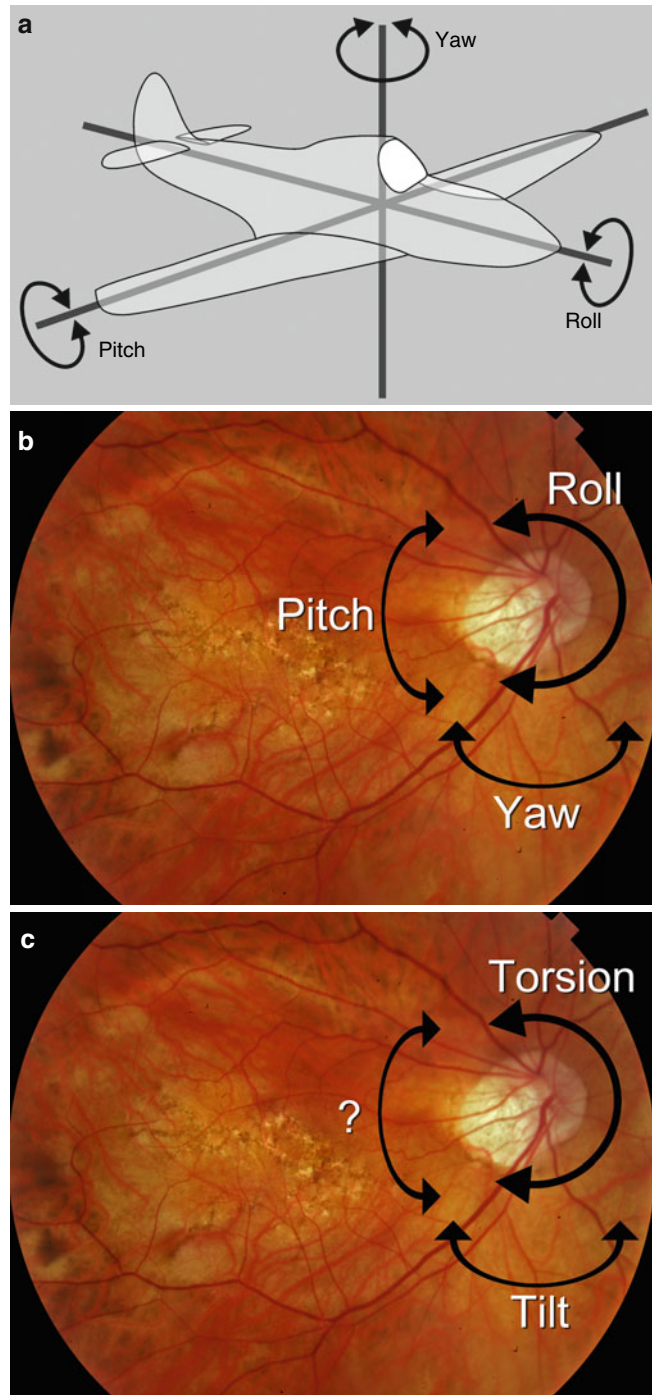


Fig. 8.9 Terminology used to describe axes of rotation. (a) With an airplane the movements around the 3 axes of rotation are termed yaw, roll, and pitch. (b) Overlaying this to optic nerve highlights the 3 axes of rotation. (c) The terminology employed in ophthalmology uses the term tilt to signify yaw, although the term also has been used to refer to what is better termed torsion, which corresponds to roll. There is no term used at present that is analogous to pitch. The imprecision induced by the lack of terminology means many authors use the term tilt to signify a variety of different things

there can be a full-thickness defect of the overlying retina. Successive OCT scans across the opening reveal retinal tissue and then also inner lamellae of sclera over the

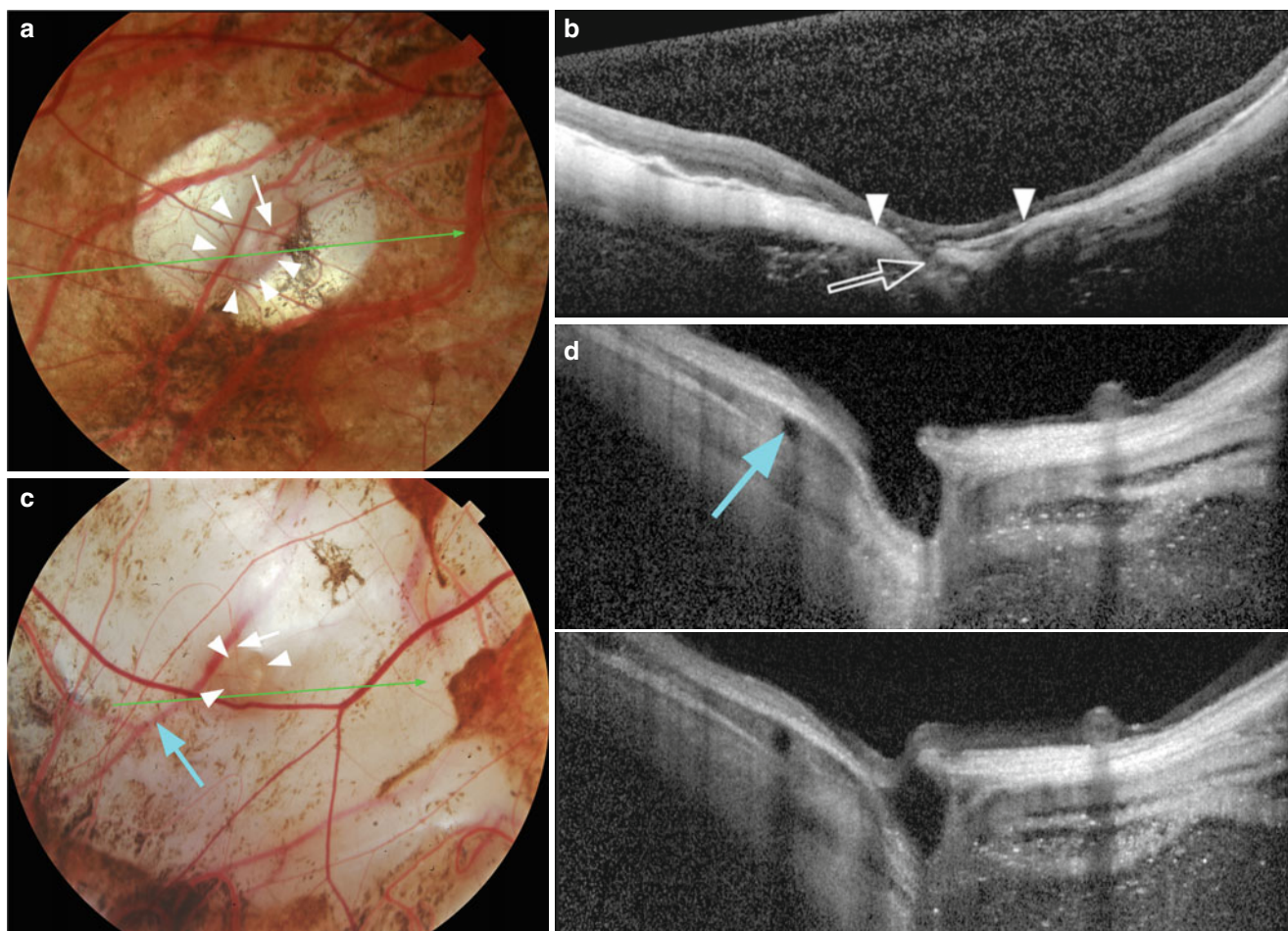


Fig. 8.10 Expansion of scleral emissary passageways and openings. (a) This patient had an oval depression (*arrowheads*) that allowed the passage of a blood vessel (*arrow*). (b) The corresponding OCT scan shows the depression between the *arrowheads* but also shows the expansion of the emissary passageway (*open arrow*) such that there was a full-thickness defect in the sclera visible. Note how thin the sclera is temporal to the opening. (c) This eye had a circular depression as

outlined by the *arrowheads*. Note the absence of the choroid and the visibility of a deeper vessel (*arrow*). (d) Upper OCT taken at the *green arrow* in (c) shows the deep depression and scleral ectasia present. The *blue arrow* points to the same vessel as that shown in (c). The lower OCT was taken slightly inferior to the upper OCT and shows retina draping across the scleral opening

passageway as the region of interest approaches the inner edge of the funnel. The draping of retinal tissue creates a closed space in which three sides are the cavity in the sclera and the roof is the retina. The addition of scleral fibers creates a true intrascleral cavitation. These exaggerated openings are found in regions where there are numerous emissaries, profound atrophy, and marked ocular expansion and thus are most commonly found near the nerve [130]. However they can be found well away from the nerve as illustrated in Fig. 8.10.

8.8.2 Irregularities of the Thinned Sclera

With ocular expansion the sclera becomes increasingly thinned, probably as the combined result of stretching and remodeling. The effects of this thinning does not appear to

be uniform, and the resultant sclera, as visualized using OCT techniques that enable deeper visualization, shows remarkable variation in thickness in many high myopes (Fig. 8.13).

8.9 Summary

This chapter reviewed the embryology, anatomy, and physiologic function of the sclera in normal eyes and examined the alterations that occur in the development of myopia and its complications. The feedback loops involved in emmetropization and myopization that involve the sclera seem to be the basis of developing myopia. Greater understanding of these processes would seem to offer the simple possibility of pharmacologic prevention of myopia, and its consequences, in the first place.

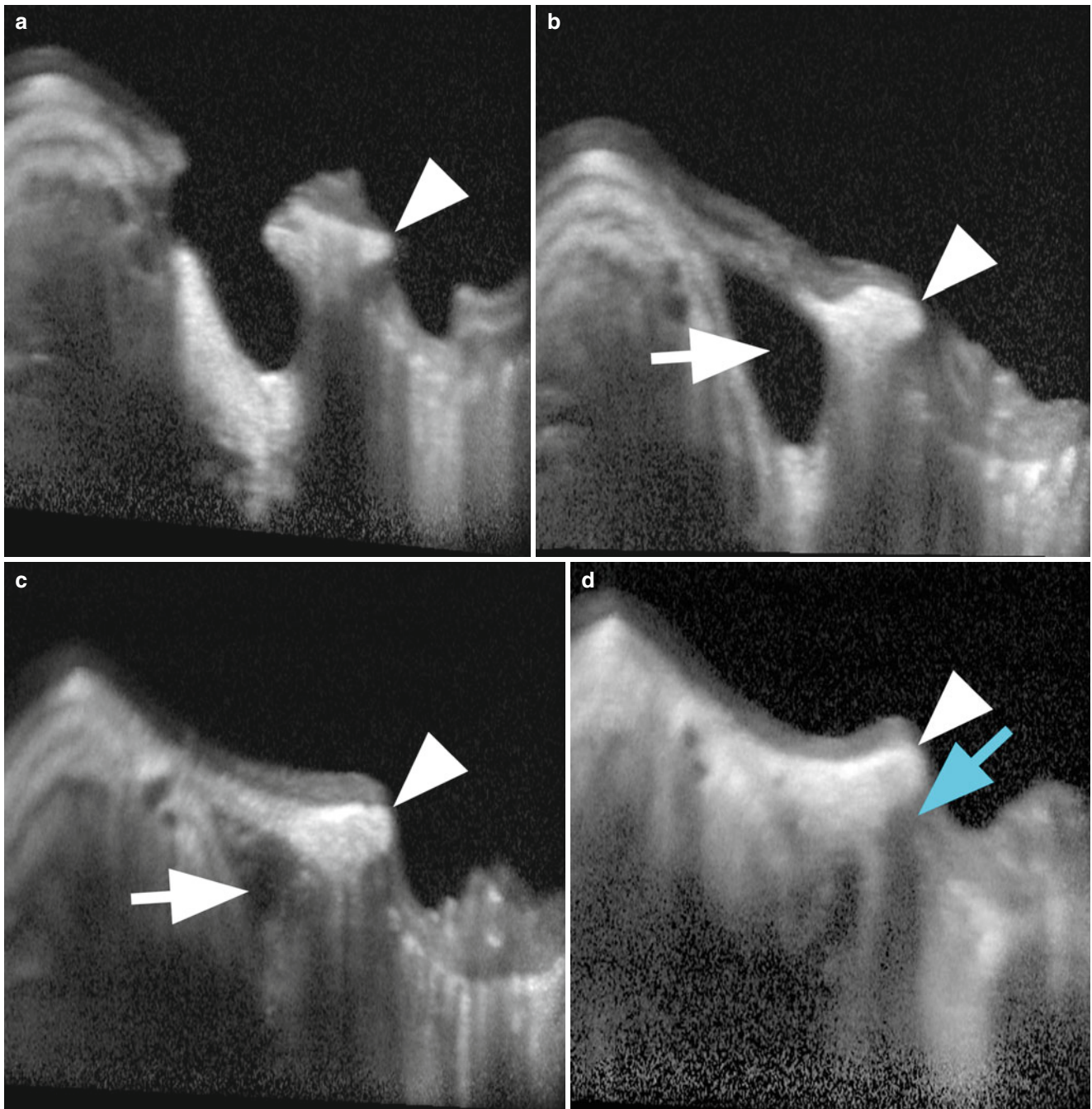


Fig. 8.11 Successive scans spaced 300 μm apart near the optic nerve in a highly myopic eye. (a) In this picture and all the remaining ones the scleral ring at the border of the optic nerve is shown by the *arrowhead*. On either side is a pit like depression. To the left is a depression related to an emissary opening and to the right is an acquired pit in the nerve.

(b) A scan taken 300 μm inferior to (a) shows a band of retinal tissue over the emissary passageway (*arrow*). (c) Inferior to (b) there appears to be scleral tissue over the passageway creating an intrascleral cavity. (d). Inferior to (c) the emissary is exposed to the outer portion of the sclera. Note the tear in the lamina cribrosa (*cyan arrow*)

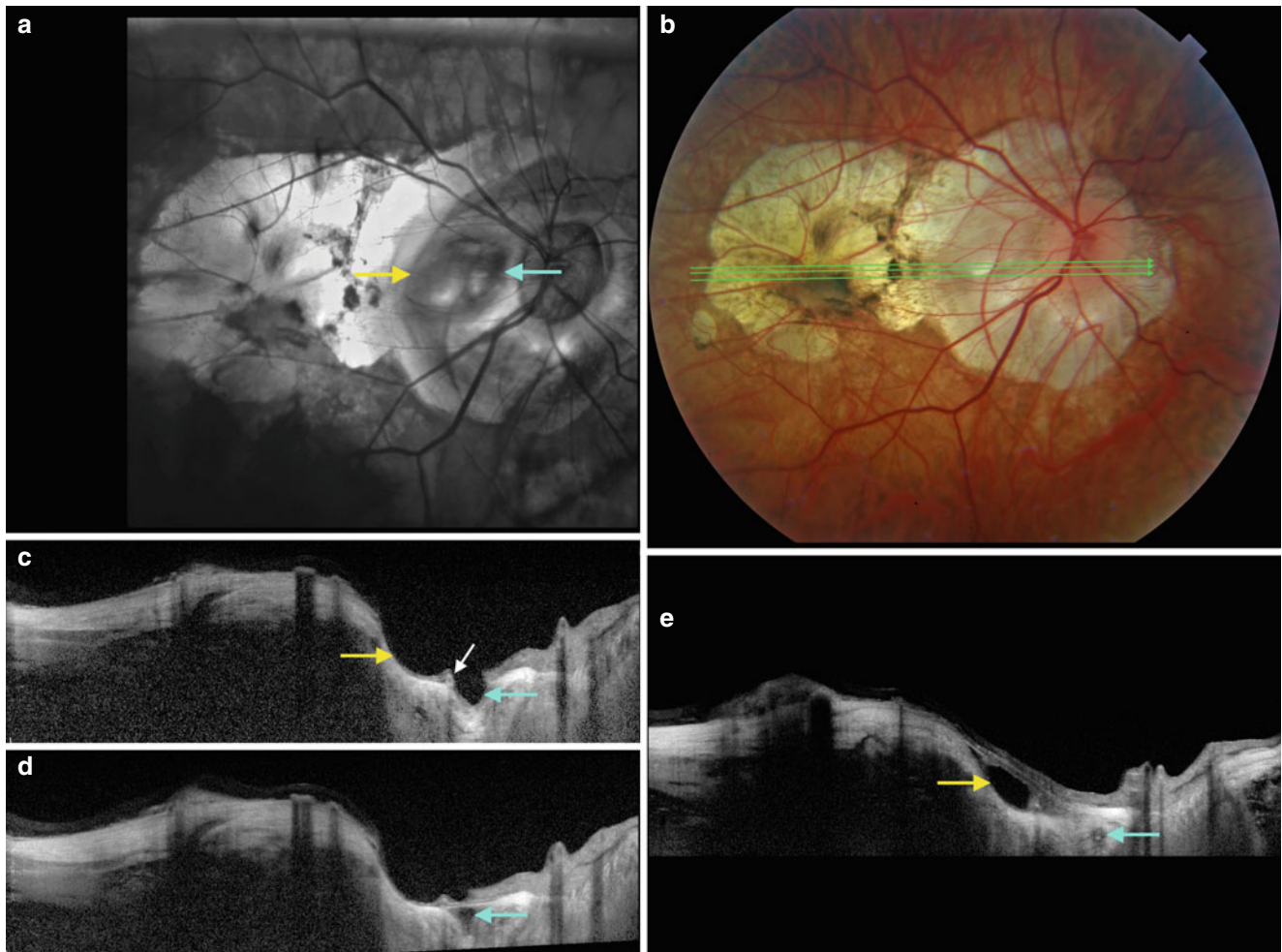


Fig. 8.12 (a) This eye shows a complex depression temporal to the nerve with two main components (*yellow and cyan arrows*) in the scanning laser ophthalmoscopic image. (b) The corresponding color fundus photograph is shown along with the scan lines shown as *green arrows*. (c) This scan corresponds to the upper scan line in (b) and shows 2 pitlike depressions; the temporal one is broader (*yellow arrow*) separated from the smaller, deeper pit (*cyan arrow*) by a ridge (*white arrow*). (d) The middle scan line in (b) shows tissue had covered the nasal pit

(*cyan arrow*) while the temporal depression remains. (e) Immediately inferior to (d) intact retina is draped over the temporal depression (*yellow arrow*). Note the continuation of the cavity seen in (d) as an intrascleral cavity in (e) as demonstrated by the *cyan arrow*. The large cavity in (e) could conceivably be mistaken for an intrachoroidal cavitation, but there is no choroid present in the region around the cavity in (e), and the mechanism of formation is different as well

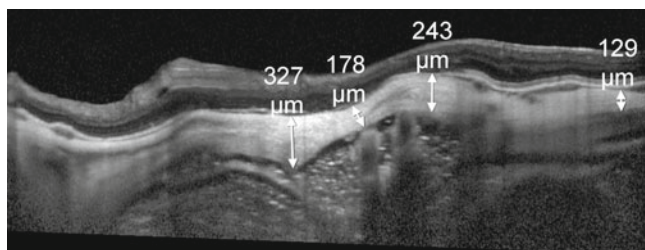


Fig. 8.13 In high myopia the posterior sclera is thinned through a process of stretching and remodeling. The remaining sclera shows a large variation in thickness

References

1. Olsen TW, Aaberg SY, Geroski DH, Edelhauser HF. Human sclera: thickness and surface area. *Am J Ophthalmol.* 1998;125(2):237–41.
2. Sellheyer K, Spitznas M. Development of the human sclera: a morphological study. *Graefes Arch Clin Exp Ophthalmol.* 1988;226:89–100.
3. Fledelius HC, Christensen AC. Reappraisal of the human ocular growth curve in fetal life, infancy, and early childhood. *Br J Ophthalmol.* 1996;80:918–21.
4. Kakizaki H, Takahashi Y, Nakano T, Asamoto K, Ikeda H, Ichinose A, Iwaki M, Selva D, Leibovitch I. Anatomy of tenon's capsule. *Clin Experiment Ophthalmol.* 2012;40(6):611–6.

5. Quigley HA, Addicks EM. Regional differences in the structure of the lamina cribrosa and their relation to glaucomatous optic nerve damage. *Arch Ophthalmol*. 1981;99(1):137–43.
6. Anderson DR. Ultrastructure of human and monkey lamina cribrosa and optic nerve head. *Arch Ophthalmol*. 1969;82(6):800–14.
7. Ko MK, Kim DS, Ahn YK. Morphological variations of the peripapillary circle of Zinn-Haller by flat section. *Br J Ophthalmol*. 1999;83(7):862–6.
8. Gauntt CD. Peripapillary circle of Zinn-Haller. *Br J Ophthalmol*. 1998;82(7):849.
9. Ko MK, Kim DS, Ahn YK. Peripapillary circle of Zinn-Haller revealed by fundus fluorescein angiography. *Br J Ophthalmol*. 1997;81(8):663–7.
10. Ohno-Matsui K, Futagami S, Yamashita S, Tokoro T. Zinn-Haller arterial ring observed by ICG angiography in high myopia. *Br J Ophthalmol*. 1998;82(12):1357–62.
11. Spitznas M. The fine structure of human scleral collagen. *Am J Ophthalmol*. 1971;71(1 Pt 1):68.
12. McBrien NA, Jobling AI, Gentle A. Biomechanics of the sclera in myopia: extracellular and cellular factors. *Optom Vis Sci*. 2009;86(1):E23–30.
13. Rada JA, Achen VR, Perry CA, Fox PW. Proteoglycans in the human sclera. Evidence for the presence of aggrecan. *Invest Ophthalmol Vis Sci*. 1997;38(9):1740–51.
14. Trier K, Olsen EB, Ammitzbøll T. Regional glycosaminoglycans composition of the human sclera. *Acta Ophthalmol (Copenh)*. 1990;68(3):304–6.
15. Watson PG, Hazleman BL, McCluskey P, Pavesio CE. Anatomical, physiological, and comparative aspects. In: Watson PG, Hazleman BL, McCluskey P, Pavesio CE, editors. *The sclera and systemic disorders*. 3rd. London: JP Medical Publishers; 2012. p. 11–45.
16. Hernandez MR, Luo XX, Igoe F, Neufeld AH. Extracellular matrix of the human lamina cribrosa. *Am J Ophthalmol*. 1987;104(6):567–76.
17. Beattie JR, Pawlak AM, McGarvey JJ, Stitt AW. Sclera as a surrogate marker for determining AGE-modifications in Bruch's membrane using a Raman spectroscopy-based index of aging. *Invest Ophthalmol Vis Sci*. 2011;52(3):1593–8.
18. Watson PG, Young RD. Scleral structure, organisation and disease. A review. *Exp Eye Res*. 2004;78(3):609–23.
19. Rada JA, Achen VR, Penugonda S, Schmidt RW, Mount BA. Proteoglycan composition in the human sclera during growth and aging. *Invest Ophthalmol Vis Sci*. 2000;41(7):1639–48.
20. Brown CT, Vural M, Johnson M, Trinkaus-Randall V. Age-related changes of scleral hydration and sulfated glycosaminoglycans. *Mech Ageing Dev*. 1994;77(2):97–107.
21. Geraghty B, Jones SW, Rama P, Akhtar R, Elsheikh A. Age-related variations in the biomechanical properties of human sclera. *J Mech Behav Biomed Mater*. 2012;16:181–91.
22. Girard MJ, Suh JK, Bottlang M, Burgoyne CF, Downs JC. Scleral biomechanics in the aging monkey eye. *Invest Ophthalmol Vis Sci*. 2009;50(11):5226–37.
23. Elsheikh A, Geraghty B, Alhasso D, Knappett J, Campanelli M, Rama P. Regional variation in the biomechanical properties of the human sclera. *Exp Eye Res*. 2010;90(5):624–33.
24. Albon J, Karwatowski WS, Avery N, Easty DL, Duance VC. Changes in the collagenous matrix of the aging human lamina cribrosa. *Br J Ophthalmol*. 1995;79(4):368–75.
25. Curtin BJ. Physiopathologic aspects of scleral stress-strain. *Trans Am Ophthalmol Soc*. 1969;67:417–61.
26. Girard MJ, Suh JK, Bottlang M, Burgoyne CF, Downs JC. Biomechanical changes in the sclera of monkey eyes exposed to chronic IOP elevations. *Invest Ophthalmol Vis Sci*. 2011;52(8):5656–69.
27. Prausnitz MR, Noonan JS. Permeability of cornea, sclera, and conjunctiva: a literature analysis for drug delivery to the eye. *J Pharm Sci*. 1998;87:1479–88.
28. Ambati J, Canakis CS, Miller JW, Gragoudas ES, Edwards A, Weissgold DJ, Kim I, Delori FC, Adamis AP. Diffusion of high molecular weight compounds through sclera. *Invest Ophthalmol Vis Sci*. 2000;41(5):1181–5.
29. Anderson OA, Jackson TL, Singh JK, Hussain AA, Marshall J. Human transscleral albumin permeability and the effect of topographical location and donor age. *Invest Ophthalmol Vis Sci*. 2008;49(9):4041–5.
30. Harada T, Machida S, Fujiwara T, Nishida Y, Kurosaka D. Choroidal findings in idiopathic uveal effusion syndrome. *Clin Ophthalmol*. 2011;5:1599–601.
31. Stewart 3rd DH, Streeten BW, Brockhurst RJ, Anderson DR, Hirose T, Gass DM. Abnormal scleral collagen in nanophthalmos. An ultrastructural study. *Arch Ophthalmol*. 1991;109(7):1017–25.
32. Jackson TL, Hussain A, Salisbury J, Sherwood R, Sullivan PM, Marshall J. Transscleral albumin diffusion and suprachoroidal albumin concentration in uveal effusion syndrome. *Retina*. 2012;32(1):177–82.
33. Mayer DL, Hansen RM, Moore BD, Kim S, Fulton AB. Cycloplegic refractions in healthy children aged 1 through 48 months. *Arch Ophthalmol*. 2001;119:1625–8.
34. Jones LA, Mitchell GL, Mutti DO, Hayes JR, Moeschberger ML, Zadnik K. Comparison of ocular component growth curves among refractive error groups in children. *Invest Ophthalmol Vis Sci*. 2005;46:2317–27.
35. Stenstrom S. Investigation of the variation and the correlation of the optical elements of human eyes. *Am J Optom Arch Am Acad Optom*. 1948;25:496–504.
36. Sorsby A, Leary GA, Fraser GR. Family studies on ocular refraction and its components. *J Med Genet*. 1966;3:269–73.
37. Zadnik K, Manny RE, Yu JA, Mitchell GL, Cotter SA, Quirarte JC, Shipp M, Friedman NE, Kleinstein RN, Walker TW, Jones LA, Moeschberger ML, Mutti DO. Ocular component data in schoolchildren as a function of age and gender. *Optom Vis Sci*. 2003;80:226–36.
38. Wildsoet CF. Active emmetropization – evidence for its existence and ramifications for clinical practice. *Ophthalmic Physiol Opt*. 1997;17(4):279–90.
39. Shen W, Vijayan M, Sivak JG. Inducing form-deprivation myopia in fish. *Invest Ophthalmol Vis Sci*. 2005;46(5):1797–803.
40. Wildsoet CF, Schmid KL. Optical correction of form deprivation myopia inhibits refractive recovery in chick eyes with intact or sectioned optic nerves. *Vision Res*. 2000;40(23):3273–82.
41. Wallman J, Adams JI. Developmental aspects of experimental myopia in chicks: susceptibility, recovery and relation to emmetropization. *Vision Res*. 1987;27:1139–63.
42. Troilo D, Gottlieb MD, Wallman J. Visual deprivation causes myopia in chicks with optic nerve section. *Curr Eye Res*. 1987;6:993–9.
43. McBrien NA, Mghaddam HO, New R, Williams LR. Experimental myopia in a diurnal mammal (*Sciurus carolinensis*) with no accommodative ability. *J Physiol*. 1993;469:427–41.
44. Andison ME, Sivak JG, Bird DM. The refractive development of the eye of the American kestrel (*Falco sparverius*): a new avian model. *J Comp Physiol A*. 1992;170:565–74.
45. Tejedor J, de la Villa P. Refractive changes induced by form deprivation in the mouse eye. *Invest Ophthalmol Vis Sci*. 2003;44:32–6.
46. Howlett MH, McFadden SA. Form-deprivation myopia in the guinea pig (*Cavia porcellus*). *Vision Res*. 2006;46:267–83.
47. Kirby AW, Sutton L, Weiss H. Elongation of cat eyes following neonatal lid suture. *Invest Ophthalmol Vis Sci*. 1982;22:274–7.
48. Sherman SM, Norton TT, Casagrande VA. Myopia in the lid-sutured tree shrew (*Tupaia glis*). *Brain Res*. 1977;124:154–7.

49. Norton TT, Essinger JA, McBrien NA. Lid-suture myopia in tree shrews with retinal ganglion cell blockade. *Vis Neurosci*. 1994; 11(1):143–53.
50. Siegwart Jr JT, Norton TT. The susceptible period for deprivation-induced myopia in tree shrew. *Vision Res*. 1998;38:3505–15.
51. McBrien NA, Lawlor P, Gentle A. Scleral remodeling during the development of and recovery from axial myopia in the tree shrew. *Invest Ophthalmol Vis Sci*. 2000;41:3713–9.
52. Wiesel TN, Raviola E. Myopia and eye enlargement after neonatal lid fusion in monkeys. *Nature*. 1977;266:66–8.
53. Smith III EL, Hung LF, Harwerth RS. Effects of optically induced blur on the refractive status of young monkeys. *Vision Res*. 1994;34:293–301.
54. Hung LF, Wallman J, Smith 3rd EL. Vision-dependent changes in the choroidal thickness of macaque monkeys. *Invest Ophthalmol Vis Sci*. 2000;41:1259–69.
55. Smith III EL, Hung LF, Huang J, Blasdel TL, Humbird TL, Bockhorst KH. Effects of optical defocus on refractive development in monkeys: evidence for local, regionally selective mechanisms. *Invest Ophthalmol Vis Sci*. 2010;51:3864–73.
56. von Noorden GK, Lewis RA. Ocular axial length in unilateral congenital cataracts and blepharoptosis. *Invest Ophthalmol Vis Sci*. 1987;28(4):750–2.
57. Wallman J, Wildsoet C, Xu A, et al. Moving the retina: choroidal modulation of refractive state. *Vision Res*. 1995;35:37–50.
58. Nickla DL, Wildsoet C, Wallman J. Compensation for spectacle lenses involves changes in proteoglycan synthesis in both the sclera and choroid. *Curr Eye Res*. 1997;16(4):320–6.
59. Troilo D, Nickla DL, Wildsoet CF. Choroidal thickness changes during altered eye growth and refractive state in a primate. *Invest Ophthalmol Vis Sci*. 2000;41:1249–58.
60. Zhu X, Park TW, Winawer J, Wallman J. In a matter of minutes, the eye can know which way to grow. *Invest Ophthalmol Vis Sci*. 2005;46(7):2238–41.
61. Schmid KL, Wildsoet CF. Effects on the compensatory responses to positive and negative lenses of intermittent lens wear and ciliary nerve section in chicks. *Vision Res*. 1996;36(7):1023–36.
62. Smith 3rd EL, Huang J, Hung LF, Blasdel TL, Humbird TL, Bockhorst KH. Hemiretinal form deprivation: evidence for local control of eye growth and refractive development in infant monkeys. *Invest Ophthalmol Vis Sci*. 2009;50(11):5057–69.
63. Diether S, Schaeffel F. Local changes in eye growth induced by imposed local refractive error despite active accommodation. *Vision Res*. 1997;37:659–68.
64. Gentle A, Liu Y, Martin JE, Conti GL, McBrien NA. Collagen gene expression and the altered accumulation of scleral collagen during the development of high myopia. *J Biol Chem*. 2003;278(19):16587–94.
65. Rada JA, Brenza HL. Increased latent gelatinase activity in the sclera of visually deprived chicks. *Invest Ophthalmol Vis Sci*. 1995;36(8):1555–65.
66. Guggenheim JA, McBrien NA. Form-deprivation myopia induces activation of scleral matrix metalloproteinase-2 in tree shrew. *Invest Ophthalmol Vis Sci*. 1996;37(7):1380–95.
67. Rada JA, Shelton S, Norton TT. The sclera and myopia. *Exp Eye Res*. 2006;82(2):185–200.
68. Schmid KL, Abbott M, Humphries M, Pyne K, Wildsoet CF. Timolol lowers intraocular pressure but does not inhibit the development of experimental myopia in chick. *Exp Eye Res*. 2000; 70(5):659–66.
69. Lin LL, Shih YF, Hsiao CK, Chen CJ, Lee LA, Hung PT. Epidemiologic study of the prevalence and severity of myopia among schoolchildren in Taiwan in 2000. *J Formos Med Assoc*. 2001;100(10):684–91.
70. Saw SM. A synopsis of the prevalence rates and environmental risk factors for myopia. *Clin Exp Optom*. 2003;86(5):289–94.
71. Lin LL, Shih YF, Hsiao CK, Chen CJ. Prevalence of myopia in Taiwanese schoolchildren: 1983 to 2000. *Ann Acad Med Singapore*. 2004;33(1):27–33.
72. He M, Zheng Y, Xiang F. Prevalence of myopia in urban and rural children in mainland China. *Optom Vis Sci*. 2009;86(1):40–4.
73. Shih YF, Chiang TH, Hsiao CK, Chen CJ, Hung PT, Lin LL. Comparing myopic progression of urban and rural Taiwanese schoolchildren. *Jpn J Ophthalmol*. 2010;54(5):446–51.
74. Saw SM, Hong RZ, Zhang MZ, Fu ZF, Ye M, Tan D, Chew SJ. Near-work activity and myopia in rural and urban schoolchildren in China. *J Pediatr Ophthalmol Strabismus*. 2001;38(3):149–55.
75. Ip JM, Rose KA, Morgan IG, Burlutsky G, Mitchell P. Myopia and the urban environment: findings in a sample of 12-year-old Australian school children. *Invest Ophthalmol Vis Sci*. 2008;49(9): 3858–63.
76. Guo Y, Liu LJ, Xu L, Lv YY, Tang P, Feng Y, Meng M, Jonas JB. Outdoor activity and myopia among primary students in rural and urban regions of Beijing. *Ophthalmology*. 2013;120(2):277–83. doi:10.1016/j.ophtha.2012.07.086.
77. Guggenheim JA, Northstone K, McMahon G, Ness AR, Deere K, Mattocks C, Pourcain BS, Williams C. Time outdoors and physical activity as predictors of incident myopia in childhood: a prospective cohort study. *Invest Ophthalmol Vis Sci*. 2012;53(6):2856–65.
78. Young FA, Leary GA, Baldwin WR, West DC, Box RA, Goo FJ, Harris E, Johnson C. Refractive errors, reading performance, and school achievement among Eskimo children. *Am J Optom Arch Am Acad Optom*. 1970;47(5):384–90.
79. Young FA, Leary GA, Baldwin WR, West DC, Box RA, Harris E, Johnson C. The transmission of refractive errors within eskimo families. *Am J Optom Arch Am Acad Optom*. 1969;46(9):676–85.
80. Tsai MY, Lin LL, Lee V, Chen CJ, Shih YF. Estimation of heritability in myopic twin studies. *Jpn J Ophthalmol*. 2009;53(6):615–22.
81. Loring EG. Are progressive myopia and conus (posterior staphyloma) due to hereditary predisposition or can they be induced by defect of refraction acting through the influence of the ciliary muscle? In: Shahurst Jr J, editor. *Transactions of the International medical congress of Philadelphia*. Philadelphia: Collins, Printer; 1877. p. 923–41.
82. Taylor CB. *Lectures on diseases of the eye*. London: Kegan Paul Trench and Co; 1891. p. 110.
83. Bedrossian RH. The effect of atropine on myopia. *Ophthalmology*. 1979;86(5):713–9.
84. McBrien NA, Moghaddam HO, Reeder AP. Atropine reduces experimental myopia and eye enlargement via a nonaccommodative mechanism. *Invest Ophthalmol Vis Sci*. 1993;34(1):205–15.
85. Fujiwara T, Imamura Y, Margolis R, Slakter JS, Spaide RF. Enhanced depth imaging optical coherence tomography of the choroid in highly myopic eyes. *Am J Ophthalmol*. 2009;148:445–50.
86. Ikuno Y, Tano Y. Retinal and choroidal biometry in highly myopic eyes with spectral-domain optical coherence tomography. *Invest Ophthalmol Vis Sci*. 2009;50(8):3876–80.
87. Nishida Y, Fujiwara T, Imamura Y, Lima LH, Kurosaka D, Spaide RF. Choroidal thickness and visual acuity in highly myopic eyes. *Retina*. 2012;32:1229–36.
88. Burke MJ, Choromokos EA, Bibler L, Sanitato JJ. Choroideremia in a genetically normal female. A case report. *Ophthalmic Paediatr Genet*. 1985;6(3):163–8.
89. Hayasaka S, Shiono T, Mizuno K, Sasayama C, Akiya S, Tanaka Y, Hayakawa M, Miyake Y, Ohba N. Gyrate atrophy of the choroid and retina: 15 Japanese patients. *Br J Ophthalmol*. 1986;70(8):612–4.
90. Sieving PA, Fishman GA. Refractive errors of retinitis pigmentosa patients. *Br J Ophthalmol*. 1978;62(3):163–7.
91. Pruett RC. Retinitis pigmentosa: clinical observations and correlations. *Trans Am Ophthalmol Soc*. 1983;81:693–735.
92. Nemet P, Godel V, Lazar M. Kearns-Sayre syndrome. *Birth Defects Orig Artic Ser*. 1982;18(6):263–8.

93. Godley BF, Tiffin PA, Evans K, Kelsell RE, Hunt DM, Bird AC. Clinical features of progressive bifocal chorioretinal atrophy: a retinal dystrophy linked to chromosome 6q. *Ophthalmology*. 1996;103(6):893–8.
94. Haegerstrom-Portnoy G, Schneck ME, Verdon WA, Hewlett SE. Clinical vision characteristics of the congenital achromatopsias. I. Visual acuity, refractive error, and binocular status. *Optom Vis Sci*. 1996;73(7):446–56.
95. Doka DS, Fishman GA, Anderson RJ. Refractive errors in patients with fundus flavimaculatus. *Br J Ophthalmol*. 1982;66(4):227–9.
96. Ohno-Matsui K, Akiba M, Modegi T, Tomita M, Ishibashi T, Tokoro T, Moriyama M. Association between shape of sclera and myopic retinohoroidal lesions in patients with pathologic myopia. *Invest Ophthalmol Vis Sci*. 2012;53(10):6046–61.
97. Cheng HM, Singh OS, Kwong KK, Xiong J, Woods BT, Brady TJ. Shape of the myopic eye as seen with high-resolution magnetic resonance imaging. *Optom Vis Sci*. 1992;69(9):698–701.
98. Atchison DA, Pritchard N, Schmid KL, Scott DH, Jones CE, Pope JM. Shape of the retinal surface in emmetropia and myopia. *Invest Ophthalmol Vis Sci*. 2005;46(8):2698–707.
99. Lim LS, Yang X, Gazzard G, Lin X, Sng C, Saw SM, Qiu A. Variations in eye volume, surface area, and shape with refractive error in young children by magnetic resonance imaging analysis. *Invest Ophthalmol Vis Sci*. 2011;52(12):8878–83.
100. Lundström L, Mira-Agudelo A, Artal P. Peripheral optical errors and their change with accommodation differ between emmetropic and myopic eyes. *J Vis*. 2009;917:1–11.
101. Schmid GF. Variability of retinal steepness at the posterior pole in children 7–15 years of age. *Curr Eye Res*. 2003;27(1):61–8.
102. Atchison DA, Jones CE, Schmid KL, Pritchard N, Pope JM, Strugnell WE, Riley RA. Eye shape in emmetropia and myopia. *Invest Ophthalmol Vis Sci*. 2004;45(10):3380–6.
103. Faria-Ribeiro M, Queirós A, Lopes-Ferreira D, Jorge J, González-Méjome JM. Peripheral refraction and retinal contour in stable and progressive myopia. *Optom Vis Sci*. 2013;90(1):9–15. doi:10.1097/OPX.0b013e318278153c.
104. Mutti DO, Sholtz RI, Friedman NE, Zadnik K. Peripheral refraction and ocular shape in children. *Invest Ophthalmol Vis Sci*. 2000;41(5):1022–30.
105. Mutti DO, Hayes JR, Mitchell GL, Jones LA, Moeschberger ML, Cotter SA, Kleinstein RN, Manny RE, Twelker JD, Zadnik K, CLEERE Study Group. Refractive error, axial length, and relative peripheral refractive error before and after the onset of myopia. *Invest Ophthalmol Vis Sci*. 2007;48(6):2510–9.
106. Logan NS, Gilmartin B, Wildsoet CF, Dunne MCM. Posterior retinal contour in adult human anisomyopia. *Invest Ophthalmol Vis Sci*. 2004;45:2152–62.
107. Seidemann A, Schaeffel F, Guirao A, Lopez-Gil N, Artal P. Peripheral refractive errors in myopic, emmetropic and hyperopic young subjects. *J Opt Soc Am A*. 2002;19:2363–73.
108. Sng CC, Lin XY, Gazzard G, Chang B, Dirani M, Chia A, Selvaraj P, Ian K, Drobe B, Wong TY, Saw SM. Peripheral refraction and refractive error in Singapore Chinese children. *Invest Ophthalmol Vis Sci*. 2011;52(2):1181–90.
109. Mutti DO, Sinnott LT, Mitchell GL, Jones-Jordan LA, Moeschberger ML, Cotter SA, Kleinstein RN, Manny RE, Twelker JD, Zadnik K, CLEERE Study Group. Relative peripheral refractive error and the risk of onset and progression of myopia in children. *Invest Ophthalmol Vis Sci*. 2011;52(1):199–205.
110. Smith III EL, Kee CS, Ramamirtham R, Qiao-Grider Y, Hung LF. Peripheral vision can influence eye growth and refractive development in infant monkeys. *Invest Ophthalmol Vis Sci*. 2005;46:3965–72.
111. Smith 3rd EL, Ramamirtham R, Qiao-Grider Y, Hung LF, Huang J, Kee CS, Coats D, Paysse E. Effects of foveal ablation on emmetropization and form-deprivation myopia. *Invest Ophthalmol Vis Sci*. 2007;48(9):3914–22.
112. Huang J, Hung LF, Smith 3rd EL. Effects of foveal ablation on the pattern of peripheral refractive errors in normal and form-deprived infant rhesus monkeys (*Macaca mulatta*). *Invest Ophthalmol Vis Sci*. 2011;52(9):6428–34.
113. Smith 3rd EL, Hung LF, Huang J. Relative peripheral hyperopic defocus alters central refractive development in infant monkeys. *Vision Res*. 2009;49(19):2386–92.
114. Tse DY, To CH. Graded competing regional myopic and hyperopic defocus produce summated emmetropization set points in chick. *Invest Ophthalmol Vis Sci*. 2011;52(11):8056–62.
115. Sng CC, Lin XY, Gazzard G, Chang B, Dirani M, Lim L, Selvaraj P, Ian K, Drobe B, Wong TY, Saw SM. Change in peripheral refraction over time in Singapore Chinese children. *Invest Ophthalmol Vis Sci*. 2011;52(11):7880–7.
116. Ferree CE, Rand G. Interpretation of refractive conditions in the peripheral field of vision. *Arch Ophthalmol*. 1933;9:925–37.
117. Williams DR, Artal P, Navarro R, McMahon MJ, Brainard DH. Off-axis optical quality and retinal sampling in the human eye. *Vision Res*. 1996;36:1103–14.
118. Guirao A, Artal P. Off-axis monochromatic aberrations estimated from double pass measurements in the human eye. *Vision Res*. 1999;39:4141–4.
119. Gustafsson J, Terenius E, Buchheister J, Unsbo P. Peripheral astigmatism in emmetropic eyes. *Ophthalmic Physiol Opt*. 2001;21:393–400.
120. Rosén R, Lundström L, Unsbo P. Sign-dependent sensitivity to peripheral defocus for myopes due to aberrations. *Invest Ophthalmol Vis Sci*. 2012;53(11):7176–82.
121. Cohen SY, Quentel G, Guiberteau B, Delahaye-Mazza C, Gaudric A. Macular serous retinal detachment caused by subretinal leakage in tilted disc syndrome. *Ophthalmology*. 1998;105:1831–4.
122. Nakanishi H, Tsujikawa A, Gotoh N, et al. Macular complications on the border of an inferior staphyloma associated with tilted disc syndrome. *Retina*. 2008;28(10):1493–501.
123. Quaranta M, Brindeau C, Coscas G, Soubrane G. Multiple choroidal neovascularizations at the border of a myopic posterior macular staphyloma. *Graefes Arch Clin Exp Ophthalmol*. 2000;238:101–3.
124. Becquet F, Ducournau D, Ducournau Y, Goffart Y, Spencer WH. Juxtapapillary subretinal pigment epithelial polypoid pseudocysts associated with unilateral tilted optic disc: case report with clinicopathologic correlation. *Ophthalmology*. 2001;108(9):1657–62.
125. Baba T, Ohno-Matsui K, Futagami S, Yoshida T, Yasuzumi K, Kojima A, Tokoro T, Mochizuki M. Prevalence and characteristics of foveal retinal detachment without macular hole in high myopia. *Am J Ophthalmol*. 2003;135(3):338–42.
126. Dałkowska A, Smogulecka E, Dziegielewska J. Retinoschisis in myopic eye. *Klin Oczna*. 1979;81(1):17–9.
127. Takano M, Kishi S. Foveal retinoschisis and retinal detachment in severely myopic eyes with posterior staphyloma. *Am J Ophthalmol*. 1999;128(4):472–6.
128. Spaide RF, Akiba M, Ohno-Matsui K. Evaluation of peripapillary intrachoroidal cavitation with swept source and enhanced depth imaging optical coherence tomography. *Retina*. 2012;32(6):1037–44.
129. Ohno-Matsui K, Akiba M, Moriyama M, Ishibashi T, Hirakata A, Tokoro T. Intrachoroidal cavitation in macular area of eyes with pathologic myopia. *Am J Ophthalmol*. 2012;154(2):382–93.
130. Ohno-Matsui K, Akiba M, Moriyama M, Shimada N, Ishibashi T, Tokoro T, Spaide RF. Acquired optic nerve and peripapillary pits in pathologic myopia. *Ophthalmology*. 2012;119(8):1685–92.
131. Cohen SY, Quentel G. Chorioretinal folds as a consequence of inferior staphyloma associated with tilted disc syndrome. *Graefes Arch Clin Exp Ophthalmol*. 2006;244:1536–8.